

THE FLORIDA STATE UNIVERSITY
COLLEGE OF ARTS AND SCIENCES

DOUBLE ENSEMBLE ESTIMATES OF PRECIPITATION IN THE
SOUTHEASTERN UNITED STATES FOR EXTREME ENSO EVENTS


By

KATHLEEN V. VERZONE


A Thesis submitted to the
Department of Meteorology
In partial fulfillment of the
requirements for the degree of
Master of Science

Degree Awarded:
Fall Semester, 1999

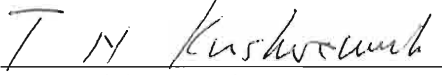
The members of the Committee approve the thesis of Kathleen V. Verzone
defended on August 3, 1999



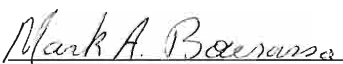
James J. O'Brien
Professor Directing Thesis



Xiaolei Zou
Committee Member



T.N. Krishnamurti
Committee Member



Mark A. Bourassa
Committee Member

ACKNOWLEDGEMENTS

I would like to thank my major professor Dr. O'Brien and my committee members Drs. Zou, Krishnamurti, and Bourassa. Special thanks to Dr. Mark Bourassa for the time he spent answering my endless questions and reading the many drafts of this thesis. I would also like to thank Drs. Tim LaRow and David Bachiochi for their help with running the model. Finally, I would like to thank my fiancé, Philip Pegion for his support and daily discussions throughout the entire course of this research.

TABLE OF CONTENTS

LIST OF FIGURES	v
ABSTRACT	iv
1. Introduction	1
2. Data	3
2.1 Synthetic Sea Surface Temperature Anomalies	3
2.2 Model Description	5
3. Design of Experiment	8
3.1 Double-ensemble	8
3.2 Selection of Events	9
3.3 Preparation of SST Anomalies for Model Input	10
4. Results	15
4.1 Single-ensemble Results	15
4.2 Double-ensemble Results	20
4.3 Warm Event minus Cold Event Differences	30
5. Conclusions	36
REFERENCES	38
BIOGRAPHICAL SKETCH	41
-----	--

LIST OF FIGURES

- 1 JMA index values for selected (a) warm and (b) cold ENSO events (solid lines) for the months of NDJF. JMA index values in (a) are for 1997-98 (dashed line) and 1982-83 (dot-dash line) warm events for NDJF. JMA index values in (b) are for 1988-89 (dashed line) and 1998-99 (dot-dash line) cold events for NDJF. In (b), JMA value for February 1998-99 is unknown, so dot-dash line is not continued. Clearly, the synthetic extreme warm events (a) are less extreme than the two shown observed extreme warm events and the synthetic extreme cold events (b) are more extreme than the two shown observed extreme cold events. 12
- 2 Synthetic SST anomalies (degrees C) for 4 selected ENSO warm events. Each row represents one series of selected SST anomalies. Extremely warm waters off the coast of Peru, which are characteristic of a warm ENSO event, are clearly shown in all four sets of SST anomalies throughout the months of DJF. 13
- 3 Same as figure 2, but for ENSO cold events. Extremely cold waters off the coast of Peru, which are characteristic of a cold ENSO event, are clearly shown in all four series of SST anomalies throughout the months of DJF. 14
- 4 Total precipitation (mm) estimates for December, January, and February for each set of warm event SSTs. All four precipitation estimates have similar spatial patterns and magnitude. Precipitation maximums are located off the coast of the Carolinas (> 700 mm) and in the Gulf of Mexico (> 700 mm). A relative minimum (< 500 mm) occurs over Florida. 16
- 5 Same as figure 4, but for cold event SSTs. Precipitation maximums are evident off the coast of the Carolinas (> 500 mm), and in the western Gulf of Mexico (> 500 mm). A relative minimum, (< 300 mm) occurs over Florida. 17

- 6 Area averaged precipitation estimates (mm per gridbox) for 19
southeastern U.S. land areas only, for each set of initial conditions
and SSTs. Precipitation estimates are for (a) warm ENSO events and
(b) cold ENSO events. The thick line indicates the ensemble average.
The error bars indicate the spread in the forecast calculated as the
average RMS difference between ensemble members and the
ensemble mean. Also shown are the observed area averaged
precipitation values for (a) the years 1982-83 (triangle) and 1997-98
(square) and (b) the years 87-88 (triangle) and 98-99 (square).
- 7 Double-ensemble precipitation totals (mm) for DJF for extreme ENSO 22
warm events. Precipitation maximums occur in the Gulf of Mexico (>
700 mm), off the coast of the Carolinas (> 800 mm), and in central
Alabama (> 700 mm). A relative minimum in precipitation occurs in
Florida (<500 mm). Minimums also occur in northwest Arkansas (<
400 mm) and into the southern tip of Florida and the Bahamas (< 400
mm).
- 8 USHCN total DJF precipitation (mm) for extreme (a) warm and (b) 23
cold ENSO events and (c) warm minus cold event precipitation totals.
Figure (a) shows a maximum in precipitation (> 600 mm) in
Mississippi and Louisiana. In (a), a precipitation minimum (< 400
mm) occurs in the peninsula of Florida. In (b), a precipitation
maximum (> 400 mm) occur in Mississippi, Alabama, and Tennessee.
Precipitation minimum occur in the peninsula of Florida (< 300 mm)
and in Arkansas (< 300 mm). Figure (c) shows a maximum (> 200
mm) in warm minus cold precipitation totals in Louisiana and
Mississippi. Warm minus cold precipitation values < 0 mm are
evident in most of Tennessee.
- 9 CMAP total DJF precipitation (mm) for ENSO warm events (1982- 25
83, 1986-87, 1987-88, 1991-92, 1997-98). A precipitation maximum
(> 600 mm) is evident in Louisiana, Mississippi, and western
Alabama. Another precipitation maximum (> 600 mm) occurs off the
coast of the Carolinas. A relative minimum occurs in the peninsula of
Florida (< 500 mm).
- 10 Same as figure 7, but for an ENSO cold event. Precipitation 26
maximums (> 500 mm) occur in the Gulf of Mexico, central Alabama,
and off the coast of the Carolinas. A relative minimum (< 400 mm)
occurs in Florida.
- 11 Same as figure 9, but for ENSO cold event of 1988-89. A 27
occurs in Florida.
- 11 Same as figure 9, but for ENSO cold event of 1988-89. A 27
precipitation maximum (> 500 mm) is centered around western
Tennessee. A band of < 200 mm of precipitation extends from the

Gulf of Mexico across Florida, into Georgia, South Carolina, and North Carolina.

- 12 Relative standard deviations (%) of ENSO (a) warm and (b) cold event double-ensemble precipitation estimates. Relative standard deviations are calculated by determining the standard deviation for each extreme event and dividing by the mean for that event. Warm event relative standard deviations are $< 25\%$ for land areas, and cold event relative standard deviations are $< 30\%$ for most land areas except for the peninsula of Florida. The double-ensemble precipitation estimates show larger relative standard deviations for extreme ENSO cold events than warm events, largely due to the smaller cold event means. 29
- 13 Double-ensemble warm minus cold event model precipitation (mm) differences for DJF. Maximums (> 200 mm) in precipitation differences occur in the Gulf of Mexico and the eastern portion of South Carolina into the Atlantic Ocean. 31
- 14 CMAP warm minus cold DJF precipitation totals (mm). A large area of maximum (> 200 mm) warm minus cold precipitation differences extends across the Gulf coast, into northern and central Florida, and across much of Georgia and South Carolina. 33
- 15 Relative uncertainty in the mean warm minus cold double-ensemble precipitation differences. Maximum ($> 40\%$) uncertainty in the mean occurs at the southern corners of the region in the Gulf of Mexico and Atlantic Ocean. For land areas, maximum ($> 15\%$) uncertainty in the mean occurs in Tennessee, stretching into northern Alabama and Mississippi. 35

ABSTRACT

Winter precipitation in the southeastern United States associated with extreme warm and cold ENSO events is examined through the use of synthetic Pacific Ocean sea surface temperature anomalies (SSTAs) and a global spectral model. A new double-ensemble technique is used to generate precipitation estimates which account for uncertainty in both the atmospheric initial conditions and sea surface temperature anomalies. The double-ensemble precipitation estimates are generated by running the FSU Global Spectral Model with an initial condition ensemble and a sea surface temperature boundary condition ensemble. The initial condition ensemble consists of ECMWF analyses from 10 days. The SSTA ensemble consists of Nov. through Feb. Pacific Ocean SSTs for four warm and four cold events. This results in a double ensemble consisting of 40 precipitation fields for each ENSO extreme.

The resulting double-ensemble precipitation estimates are compared to both in-situ and satellite data. These precipitation estimates agree well with observations in both spatial pattern and magnitude. They indicate, in agreement with observations, that on average the southeastern United States receives more precipitation during ENSO warm event winters than during ENSO cold event winters. The double ensemble area average winter precipitation totals for the southeastern United States from the double-ensemble winter (December, January, and February) precipitation totals range from a maximum of winter precipitation totals for the southeastern United States from the double-ensemble winter (December, January, and February) precipitation totals range from a maximum of 359 mm during an extreme warm event and a minimum of 239 mm during an extreme

cold event, indicating a 50% increase in precipitation in the southeastern U.S. from an extreme cold event to an extreme warm event.

There is considerable case to case variability within the ensemble, which supports the need for an ensemble approach. The spread in DJF total precipitation estimates and the uncertainty in the mean difference from warm to cold events is calculated and found to be sufficiently small over land, indicating excellent confidence in the double-ensemble precipitation estimates.

1. INTRODUCTION

Ensemble forecasting has been used to generate improved NWP forecasts by considering the uncertainty in the initial conditions of the atmosphere. Stenstrund et al. (1999) used 10 member ensembles from the Meso Eta Model to forecast cyclone positions. Zhang and Krishnamurti (1999) showed how the ensemble technique could be used to improve hurricane forecasts. Barnett (1995) performed a “monte-carlo” climate forecast in which he determined that a 10 member ensemble is the minimum number of ensembles necessary for climate forecasting. Ensemble forecasting has also been applied to El Niño-Southern Oscillation (ENSO) prediction using a coupled ocean-atmosphere system (LaRow and Krishnamurti 1999). There are many other examples of ensemble forecasts. This study uses a new “double-ensemble” technique to estimate winter precipitation in the southeastern United States during extreme warm and cold ENSO events. This new technique is utilized to consider uncertainties in both the initial conditions for the atmosphere and sea surface temperature (SST) anomalies for extreme warm and cold ENSO events.

Previous studies (Sittel 1994; Green 1994) have shown a teleconnection between SSTs in the equatorial Pacific Ocean associated with ENSO and winter precipitation patterns in the southeastern United States. These studies show that the southeastern U.S. receives more rainfall than normal during a warm event winter and less rainfall during a

cold event winter. This changing precipitation pattern is attributed to the altered 850 hPa and 300 hPa mean wind flow (Smith et al. 1998). During a warm event winter, 850 hPa and 300 hPa wind patterns are altered to maintain a flow of moisture over the Gulf of Mexico, which enhances precipitation. By contrast, during a cold event winter, the 850 hPa and 300 hPa mean wind fields restrict flow to only the western portion of the Gulf of Mexico, thereby providing less moisture and uplift in the southeastern U.S. and suppressing precipitation. This study investigates the teleconnection between SSTs and winter precipitation in the southeastern U.S. for extreme ENSO events.

The “double-ensemble” technique requires both an ensemble of initial atmospheric conditions and an ensemble of SSTs for extreme ENSO events. Since the short historical record of SSTs provides few extreme ENSO events, synthetic SSTs (Caron and O’Brien 1998; section 2.1) are used. These synthetic SSTs are used as boundary conditions for the Florida State University Global Spectral Model (FSUGSM; section 2.2) for the purpose of investigating the impacts of extreme ENSO events on winter precipitation in the southeastern United States. Descriptions are given for the double-ensemble technique, selection of extreme ENSO events used to force the model, and preparation of the synthetic SSTs for input into the model (section 3). The resulting double-ensemble precipitation estimates are validated in comparisons to in situ and satellite observation (section 4). Finally, conclusions (section 5) discuss the effectiveness of the double-ensemble technique for estimating winter precipitation in the southeastern United States for extreme warm and cold events. The double-ensemble method provides excellent estimates of the spread in precipitation for both phases of ENSO in the United States for extreme warm and cold events. The double-ensemble method provides excellent estimates of the spread in precipitation for both phases of ENSO in the southeastern United States.

2. DATA

Synthetically generated sea surface temperature anomalies (Caron and O'Brien 1998) for extreme ENSO events are used as input for a global spectral model. The generation of the synthetic sea surface temperature anomalies is described below (section 2.1). The FSU Global Spectral Model is used for producing the precipitation forecasts (Cocke and LaRow 1999). The basic model physics are briefly mentioned (section 2.2) with a more detailed description of the precipitation schemes.

2.1 Synthetic Sea Surface Temperature Anomalies

Synthetic sea surface temperature anomalies (SSTAs) for the Equatorial Pacific Ocean (31S-27N and 121E-71W) are generated using the Caron and O'Brien (1998) sea surface temperature anomaly generator. Each run of the SSTA generator produces a 40 year set of monthly SSTAs for the Equatorial Pacific Ocean on a 2°x2° grid. Caron and O'Brien have shown that adding the synthetic SSTAs to climatological SSTs (Smith et. al. 1996) results in SSTs which are statistically indistinguishable from observation based data sets. The synthetic data have a probability structure essentially identical to the observed data.

The generation of synthetic SSTAs is accomplished through frequency domain

The generation of synthetic SSTAs is accomplished through frequency domain modeling. The amplitude spectra of the Fourier transformed time series for each spatial

EOF of the Smith et al. (1996) SSTs were determined to consist of physical processes (ENSO, quasibiennial, and decadal oscillations), red noise, and/or white noise. These physical processes were present in the amplitude spectra of the Fourier coefficients from the first two principle components (PCs). The amplitude peaks in the spectra of the first two PC's are modeled using a rescaled Maxwell probability density function (PDF; PC1) and a rescaled Rayleigh PDF (PC2) to represent the amplitude peaks corresponding to physical processes. Additionally, the rest of the amplitude of the first two PC's is modeled as red and white noise. Prior to modeling the physical components, the spectra for red and white noise were subtracted from the observed spectra. Principle components 3-11 are modeled as red noise (related to the autocovariance of monthly SSTs) and white noise (variance associated with uncorrelated noise). The amplitude spectra of the final 469 principle components were determined to be well approximated as random, and they are modeled as white noise by a single PC. The phase of the reconstructed Fourier transform is initialized with random numbers from a uniform distribution. The amplitude spectra of the three modeled contributions (physical processes, red noise, and/or white noise) are added in a root-mean-square sum to preserve the variance of the time series.

For each PC, a model Fourier series is generated from the product of the model amplitude and the complex exponential of a random phase. An inverse Fourier transform is applied to determine each time series. Products of the spatial and temporal parts of the modeled principle components are summed, providing a 40 year set of monthly synthetic SST anomalies for the Equatorial Pacific Ocean.

SST anomalies for the Equatorial Pacific Ocean.

2.2 Model Description

The FSUGSM (Krishnamurti et al. 1989) is used in this study to estimate precipitation during extreme ENSO events. It has a resolution of 63 waves in the horizontal (T63) and 14 unevenly spaced sigma levels in the vertical. This corresponds to approximately 1.8° latitude by 1.8° longitude resolution. The modeled physics include large-scale condensation (Kanamitsu 1975), deep convection (Pan and Wu 1994), dry convective adjustment, radiative fluxes based on a band model (Hashvardan and Corsetti 1984; Lacis and Hansen 1974), shallow convection (Tiedke 1984), surface energy balance coupled to similarity theory (Krishnamurti et al. 1991), vertical diffusion (Louis 1979), fourth-order horizontal diffusion (Kanamitsu et al. 1983), parameterization of low, middle, and high clouds, and a diurnal cycle. Detailed descriptions of these parameterizations can be found in Manobianco (1988) and Krishnamurti (1995). The model has been found to produce too much precipitation over the ocean (LaRow, personal communication).

Modeled precipitation is generated through large-scale condensation and deep convection. Large-scale condensation occurs as a result of the removal of supersaturation due to dynamic ascent of absolutely stable saturated air. The air rises and cools until supersaturation occurs. Water vapor is condensed out as non-convective precipitation, and the appropriate heat release occurs in that level of the atmosphere.

The deep convection scheme used in this study is a simplified Arakawa-Schubert scheme (Pan and Wu 1994). Points for potential convection are first located by selecting the grid points with maximum values of moist static energy in the column below 700 hPa (Pan and Wu 1994). Points for potential convection are first located by selecting the grid points with maximum values of moist static energy in the column below 700 hPa. The level of maximum moist static energy is determined to be the updraft origin. A

parcel is lifted from the updraft origin to the level of free convection (LFC), which is the cloud base. Convection is allowed when the depth of the layer between the updraft origin and the LFC remains less than 150 hPa. At the LFC, 50% of the cloud mass is taken from the updraft origin. The other half of the cloud mass is modified due to entrainment into the parcel below the cloud base. Once the cloud base is reached, the parcel continues to rise, without entrainment from the environment, up to the level of neutral buoyancy. The level of neutral buoyancy determines the cloud top. At the cloud top, all of the cloud mass flux is detrained to the environment.

The intensity of the convection is determined by creating a closed parameterization. This condition is achieved through Arakawa and Schubert's (1974) quasi-equilibrium hypothesis that large-scale processes in the atmosphere are nearly balanced by stabilization due to sub grid scale cumulus clouds. Arakawa and Schubert quantified stabilization and destabilization by defining a cloud work function which measures the vertically integrated buoyancy. Although, Arakawa and Schubert use a multi-scale ensemble, only the cloud with the deepest convection is used for this simplified scheme. The cloud work function is calculated for this single cloud and used to quantify the ability of the large-scale environment to maintain convection. The large-scale environment is allowed to respond to the sub-gridscale convection through entrainment, detrainment, and cloud mass flux, which effect the moist static energy and moisture of the large-scale environment.

Convective rain is parameterized by converting a portion of the cloud liquid water into precipitation. The condensed water vapor in both the downdraft and undraft are

Convective rain is parameterized by converting a portion of the cloud liquid water into precipitation. The condensed water vapor in both the downdraft and updraft are

accumulated from cloud top to the surface to determine the amount of convective precipitation. Evaporation is considered for rain falling through unsaturated layers.

3. DESIGN OF EXPERIMENT

The most extreme warm and cold ENSO events are selected from a limited number of synthetic SSTA realizations for input into the FSUGSM. Multiple SST conditions and multiple initial conditions for the atmosphere produce a double-ensemble forecast of precipitation for the entire globe for extreme ENSO events. The region of interest is the southeastern United States (24N-37N and 95W-75W); therefore the precipitation forecast for this region is extracted out of the global forecast. A description of the double-ensemble method is given below (section 3.1). The selection of the extreme ENSO events that are used as input into the model and the preparation of this data for input into the FSUGSM are also described (section 3.2).

3.1 Double-Ensemble

A double-ensemble technique is used to determine the atmospheric response to extreme warm/cold synthetic ENSO events in the form of winter precipitation in the southeastern United States. The SST ensembles consist of 4 sets of SSTs for each ENSO extreme, which differ only in the equatorial Pacific Ocean (31S-27N and 121E-71W). The atmospheric initial conditions ensemble consists of 10 different cases obtained from the European Center for Medium Range Weather Forecasting (ECMWF). These initial conditions are 12 UTC ECMWF analyses: October 31-November 3, 1987; October 30-November 3, 1988; and November 1, 1995.

The FSUGSM is run for the four model months of November, December, January, and February. November is a “spin-up” month, allowing for the atmosphere to adjust to the SSTs. The DJF seasonally totaled model precipitation is averaged for all 10 atmospheric initial conditions, thereby producing an ensemble averaged forecast for each of the 4 warm and 4 cold events. Averaging the atmospheric ensembles for the four extreme warm/cold ENSO SSTs produces a double-ensemble estimate. This double-ensemble estimate accounts for both uncertainties in the initial conditions of the atmosphere and uncertainties in the SSTs between various extreme warm/cold ENSO events.

3.2 Selection of Events

This study selects one extreme warm and one extreme cold event from each of four sets of synthetic SSTAs. Warm and cold events are determined through the JMA index (Japan Meteorological Agency 1991). It is a 5-month running mean of the SST anomalies for the region 4S-4N and 150-90W. A warm event is considered to occur when the JMA index is $\geq 0.5^{\circ}$ C for at least 6 consecutive months. A JMA index $\leq -0.5^{\circ}$ C for at least 6 consecutive months defines a cold event. There is additional JMA criteria that October-December are three of the six months; however, this is not applied since the synthetic SSTAs do not correspond to specific months. Once the modified JMA index is calculated for each of the sets of synthetic SSTAs and warm and cold events are identified in each set, the most extreme events are easily identified (Table 1).

Although the selected ENSO events are the most extreme events generated from a limited number of realizations of the SST anomaly generator, they do not necessarily represent the most extreme events observed historically. The warm events selected are

not as extreme as the recent extreme events of 1982-83 and 1997-98 (Fig 1a). By contrast, the simulated extreme cold events are more extreme than the observed cold events of 1988-1989 and 1998-1999 (Fig 1b).

3.3 Preparation of SST Anomalies for Model Input

The SSTs for selected warm and cold events need to be prepared for input into the model. These synthetic warm and cold events do not explicitly correspond to any particular month or year. However, a representative month must be attached to these events prior to model input. Since most warm/cold events peak in December (Rasmussen and Carpenter 1982), the peak of each synthetic warm/cold event (determined by max/min JMA index value) is assigned the month December. The 4 months of November, December, January and February are extracted to be used as model input (Figs. 2 & 3).

The synthetic SSTAs must be added to climatology to create SSTs for model input. Although the synthetic SSTAs are generated only for the Equatorial Pacific Ocean, the model is global and requires global SSTs as input. This raises the potential problem of discontinuities at the edges of the Equatorial Pacific region. Therefore, the synthetic SSTAs are filtered using a hyperbolic tangent filter prior to adding the Smith et al. (1996) global monthly SST climatology. Finally, these monthly global SST fields for each synthetic event are interpolated to the T63 gaussian grid and weekly fields for input into the model.

Table 1. Maximum/minimum JMA Index values for each selected synthetic warm/cold events.

Set Number	Warm Events (°C)	Cold Events (°C)
1	1.89	-2.45
2	2.32	-1.65
3	2.52	-1.77
4	2.57	-1.76

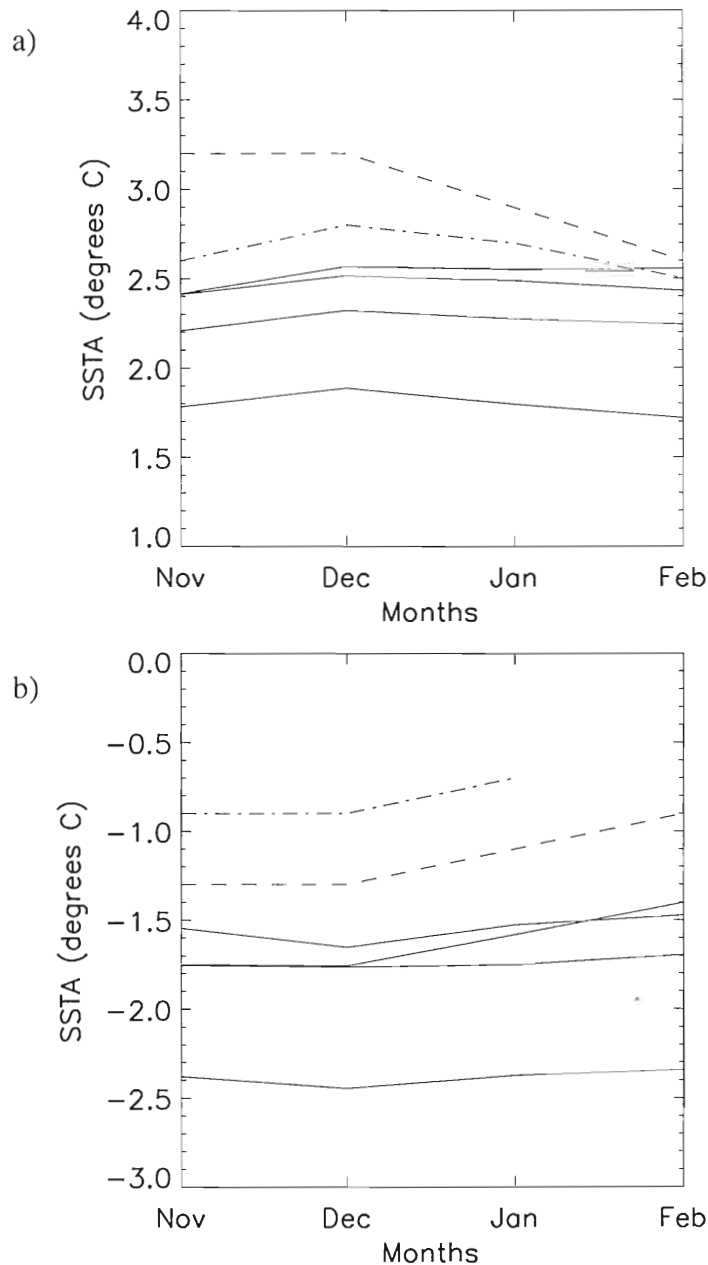


Fig. 1. JMA index values for selected (a) warm and (b) cold ENSO events (solid lines) for the months of NDJF. JMA index values in (a) are for 1997-98 (dashed line) and 1982-83 (dot-dash line) warm events for NDJF. JMA index values in (b) are for 1988-89 (dashed line) and 1998-99 (dot-dash line) cold events for NDJF. In (b), JMA value for February 1998-99 is unknown, so dot-dash line is not continued. Clearly, the synthetic extreme warm events (a) are less extreme than the two shown observed extreme (cold-dash line) cold events for NDJF. In (b), JMA value for February 1998-99 is unknown, so dot-dash line is not continued. Clearly, the synthetic extreme warm events (a) are less extreme than the two shown observed extreme warm events and the synthetic extreme cold events (b) are more extreme than the two shown observed extreme cold events.

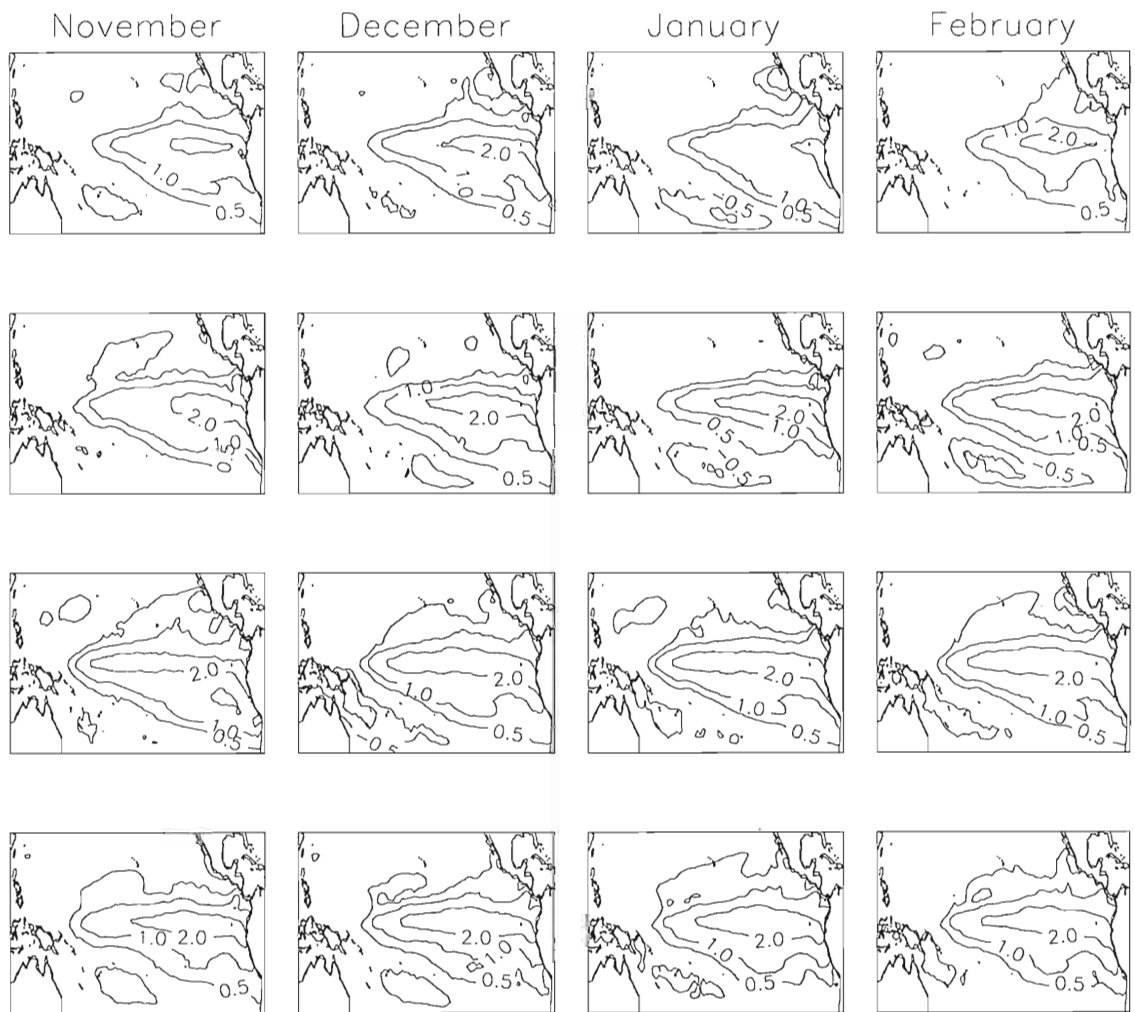


Fig. 2. Synthetic SST anomalies (degrees C) for 4 selected ENSO warm events. Each row represents one series of selected SST anomalies. Extremely warm waters off the coast of Peru, which are characteristic of a warm ENSO event, are clearly shown in all four sets of SST anomalies throughout the months of DJF.

event, are clearly shown in all four sets of SST anomalies throughout the months of DJF.

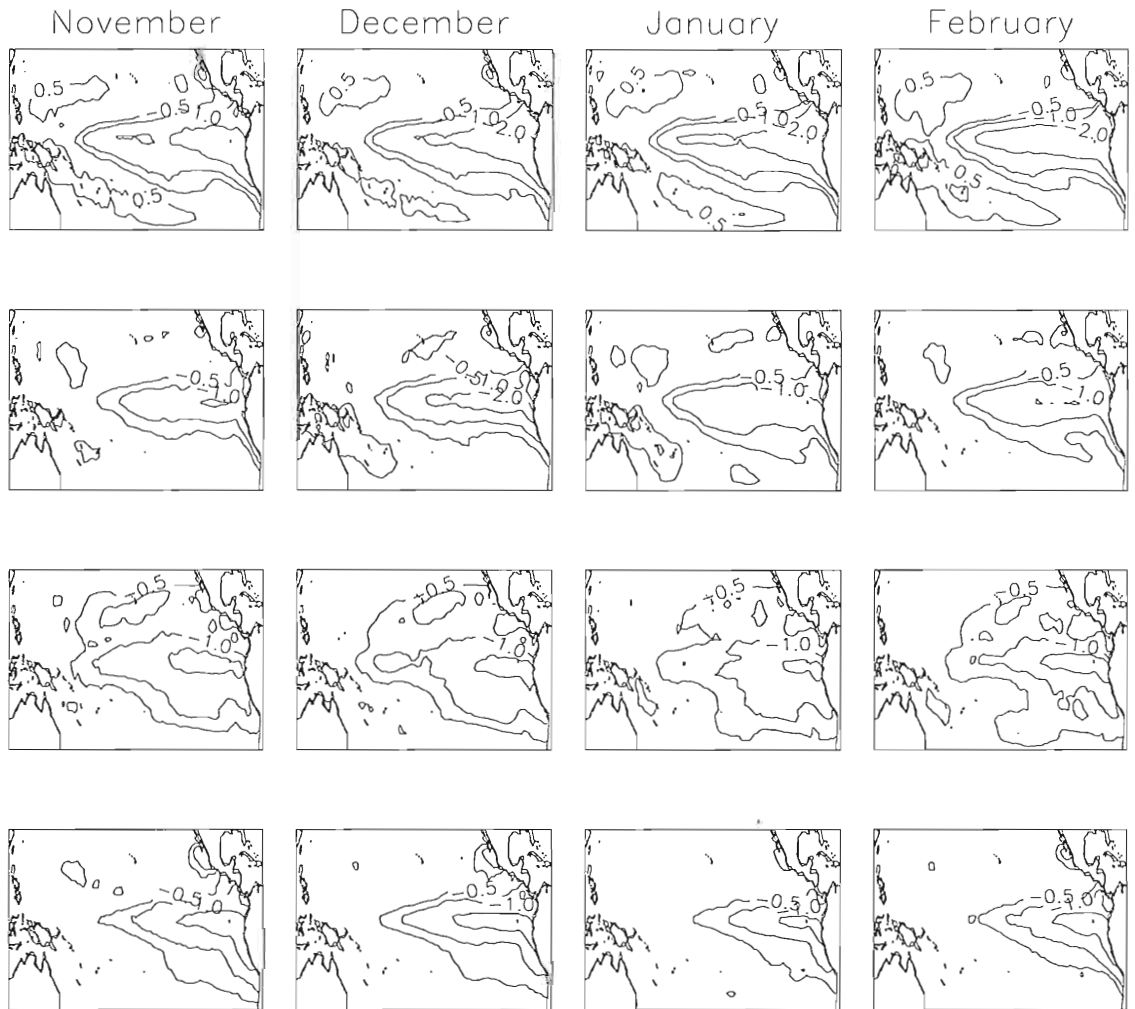


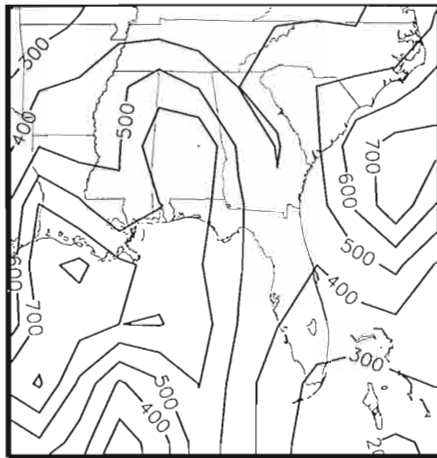
Fig. 3. Same as figure 1, but for ENSO cold events. Extremely cold waters off the coast of Peru, which are characteristic of a cold ENSO event, are clearly shown in all four series of SST anomalies throughout the months of DJF.

4. RESULTS

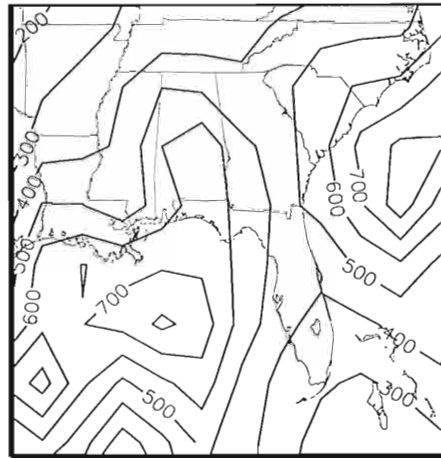
4.1 Single-ensemble Results

The total winter precipitation estimates from the FSUGSM are first examined as single-ensemble averages from the 10 different atmospheric initial conditions. These single-ensemble results produce 4 precipitation estimates for warm events and 4 precipitation estimates for cold events. For each of the four sets of SSTs, the ensemble precipitation estimate produces similar results in both magnitude and spatial pattern for each ENSO warm event (Fig. 4). Likewise, for cold events, the precipitation estimates for each of the 4 sets of SSTs have a similar pattern and magnitude (Fig. 5). It is also evident that these modeled precipitation estimates for the southeastern U.S. indicate drier winters during extreme cold events than during extreme warm events, as is generally observed (Sittel 1994; Green 1997).

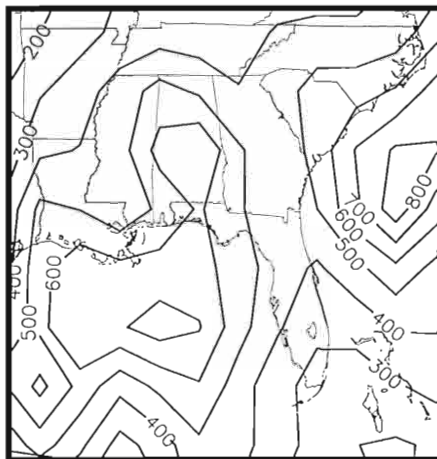
It is important to consider the spread in the precipitation forecasts between the differing sets of initial conditions for the atmosphere. The spread is defined as the root mean square (RMS) distance between ensemble members and the ensemble mean (Whitaker and Lough 1998). This spread indicates the uncertainty in the precipitation estimates over land for events with the same SSTs in the equatorial Pacific Ocean (EQPAC) and different initial conditions in the atmosphere. This spread can be used as a measure of the skill of the ensemble forecast (Whitaker and Lough 1998). The spread



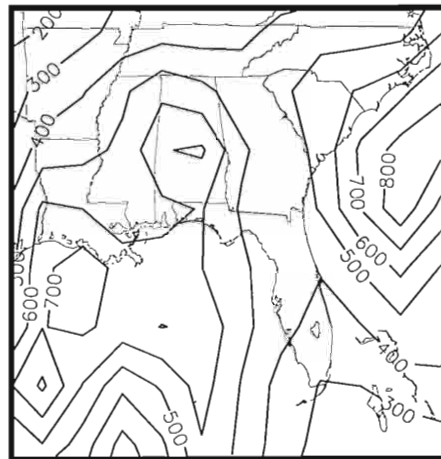
(a) SST Set 1



(b) SST Set 2

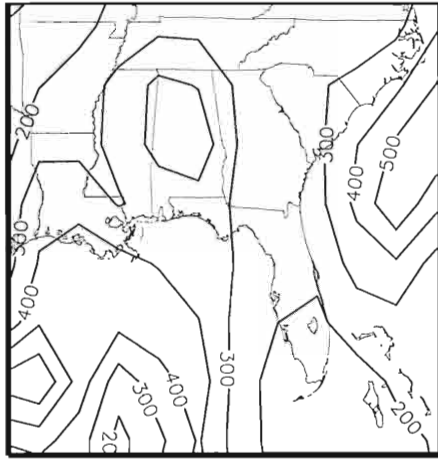


(c) SST Set 3

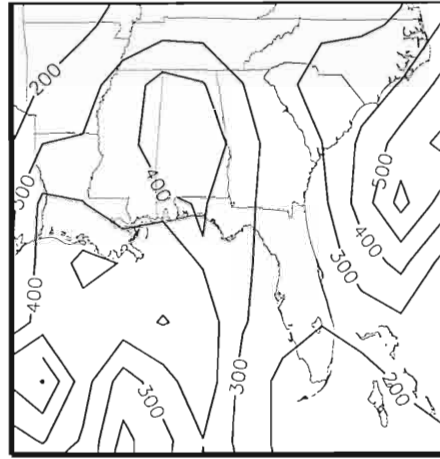


(d) SST Set 4

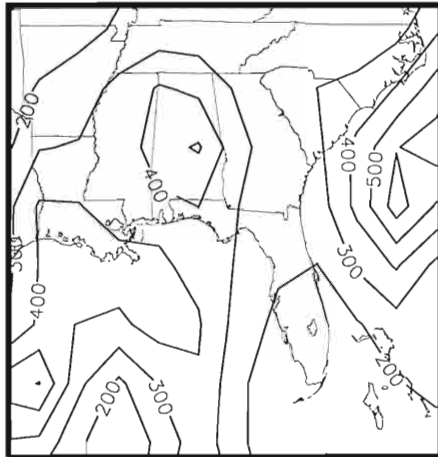
Fig. 4. Total precipitation (mm) estimates for DJF for each set of warm event SSTs. All four precipitation estimates have similar spatial patterns and magnitude. Precipitation maximums are located off the coast of the Carolinas (>700 mm) and in the Gulf of Mexico (>700 mm). A relative minimum (<500 mm) occurs over Florida.



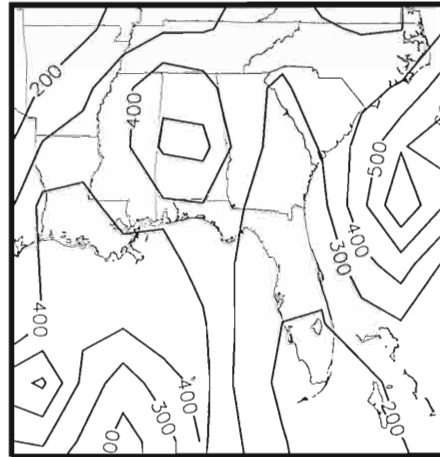
(a) SST Set 1



(b) SST Set 2



(c) SST Set 3



(d) SST Set 4

Fig. 5. Same as figure 3, but for cold event SSTs. Precipitation maximums are evident off the coast of the Carolinas (> 500 mm), and in the western Gulf of Mexico (> 500 mm). A relative minimum (< 300 mm) occurs over Florida.

of the warm event area averaged total precipitation estimates for December, January, and February (DJF) over land (indicated by error bars in Fig. 6a) ranges from about ± 32.2 mm to approximately ± 57.5 mm. The spread in the DJF land area averaged precipitation estimates for cold events (indicated by error bars in Fig. 6b) ranges from ± 42.6 mm to ± 55.5 mm. Based on the land area averaged DJF precipitation estimates, an individual warm (cold) event can be drier (wetter) than an individual cold (warm) event. However, once the ensemble average is calculated (indicated by the line in Fig. 6), it is clear that on average the model estimates more precipitation during a warm event winter than during a cold event winter. This result is supported by Sittel (1994) and Green (1997), which demonstrate with in-situ data that the southeastern United States is drier during an average cold event winter than during an average warm event winter.

The most extreme simulated events provide a guide for determining how much (little) precipitation can occur during the most extreme warm (cold) event winter in the southeastern United States. This “envelope”, determined by the ensemble precipitation estimates, indicates that for the most extreme warm event, no more than 475 mm of rain occurs in the southeastern United States and for the most extreme cold event, no less than 140 mm of precipitation occurs in the southeastern United States. These extreme precipitation estimates are wetter (in the warm event case) and drier (in the cold event case) than have been observed (Fig. 6). The extremes or outliers (Fig. 6) are not produced by one particular set of initial conditions, thereby supporting an ensemble approach to modeling precipitation.

approach to modeling precipitation.

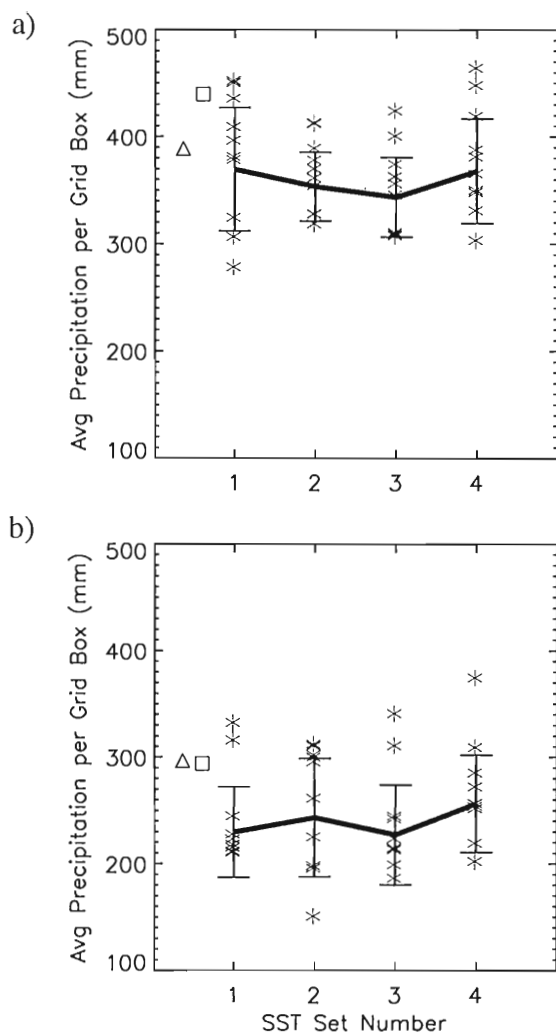


Fig. 6. Area averaged precipitation estimates (mm per grid box) for the southeastern U.S. land areas only, for each set of initial conditions and SSTs. Precipitation estimates are for (a) warm ENSO events and (b) cold ENSO events. The thick line indicates the ensemble average. The error bars indicate the spread in the forecast calculated as the RMS difference between ensemble members and the ensemble mean. Also shown are the observed area averaged precipitation values for (a) the years 1982-83 (triangle) and 1997-98 (square) and (b) the years 1987-88 (triangle) and 1998-99 (square).

Although the extreme simulated events encompass the range of all observed events, the ensemble averaged precipitation estimates do not. The ensemble precipitation averages for extreme warm events indicate less precipitation than was observed in the 1982-83 and 1997-98 extreme ENSO warm events. This can be attributed to the fact that the simulated warm events were not as extreme as either the 1982-83 or 1997-98 ENSO warm events. By contrast, the ensemble precipitation averages for extreme cold events indicates much drier conditions in the southeastern United States than has been observed in the extreme ENSO cold events of 1988-89 and 1998-99. This can be explained by the fact that the simulated cold events are more extreme than either of the indicated observed cold events.

4.2 Double-Ensemble Results

The single-ensemble precipitation estimates provide similar representations of precipitation in the southeastern United States warm and cold event winters for each set of SSTs. Each single-ensemble forecast produces results, which account for the variability in precipitation due to differing atmospheric initial conditions. However, estimates of precipitation amounts in the southeastern United States during extreme warm and cold events must also consider SST variability. Therefore, double-ensemble averaged precipitation estimates are determined for both warm and cold events. They are validated by comparison to the Historical Climate Network (HCN; Karl et al. 1990) station data and the CPC Merged Analysis of Precipitation (CMAP; Xie and Arkin

1997).

4.2.1 Warm Event

A double-ensemble winter precipitation estimate (Fig. 7) is generated for extreme ENSO warm events. The most notable features of this precipitation estimate are the areas of maximum rainfall in the Gulf of Mexico and off the coast of the Carolinas, and the minimum of precipitation in the peninsula of Florida. The two maxima indicate seasonal rainfall estimates greater than 700 mm over the oceans and greater than 600 mm of precipitation over land.

The double-ensemble averaged precipitation estimate is compared with station observations from extreme warm events. The United States Historical Climate Network (USHCN) data set provides monthly averaged precipitation totals for a variety of stations for the years 1946-1997 (Karl et al. 1990). Since this study focuses on extreme warm/cold events, the winters of 1972-73 and 1982-83 are selected as the two most extreme warm events (based on the JMA index values) within the data set, and are compared to the double-ensemble precipitation estimate. It is clear from this comparison that the double-ensemble precipitation estimates (Fig. 7) have a very similar pattern to observations (Fig. 8a). The larger amount of precipitation in Louisiana, Mississippi, Alabama, Georgia, and the Florida panhandle is captured well by the model estimate. However, there is some discrepancy between the model and the USHCN station data in the Carolinas where the model appears to predict more rain. Similarly, the model correctly shows the peninsula of Florida to be drier than the panhandle and southern Georgia; however, the model precipitation estimates for the peninsula of Florida are much higher than the USHCN station data. This is likely due to the fact that the FSUGSM at T63 resolution considers most of the peninsula of Florida to be ocean.

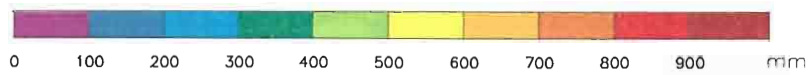
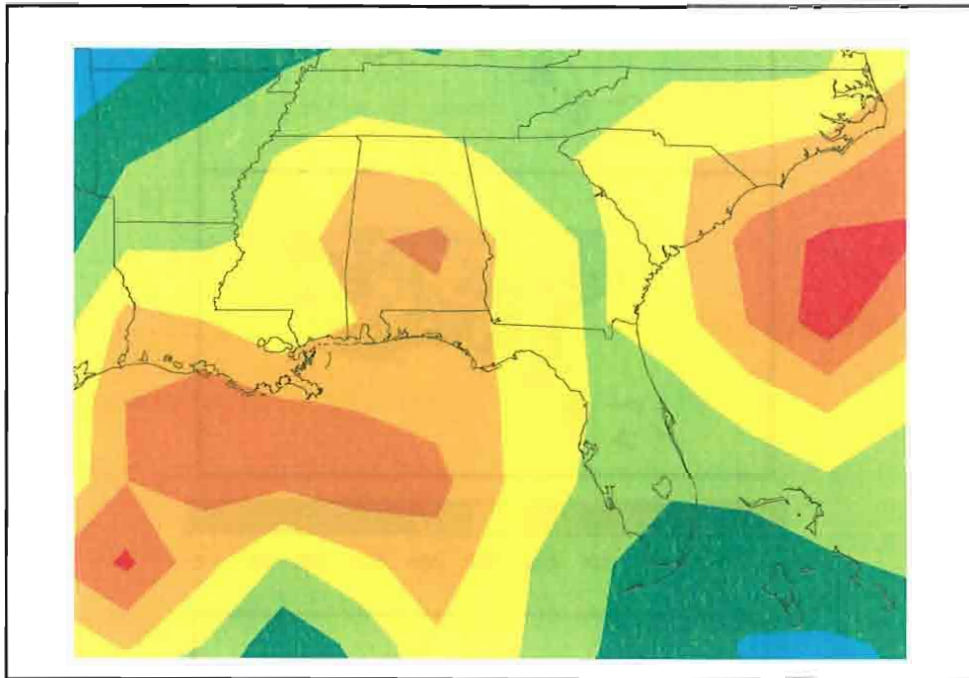


Fig. 7. Double ensemble precipitation totals (mm) for DJF for extreme ENSO warm events. Precipitation maximums occur in the Gulf of Mexico (> 700 mm), off the coast of the Carolinas (> 800 mm), and in central Alabama (> 700 mm). A relative minimum in precipitation occurs in Florida (< 500 mm). Minimums also occur in northwest Arkansas (< 400 mm) and into the southern tip of Florida and the Bahamas (< 400 mm).

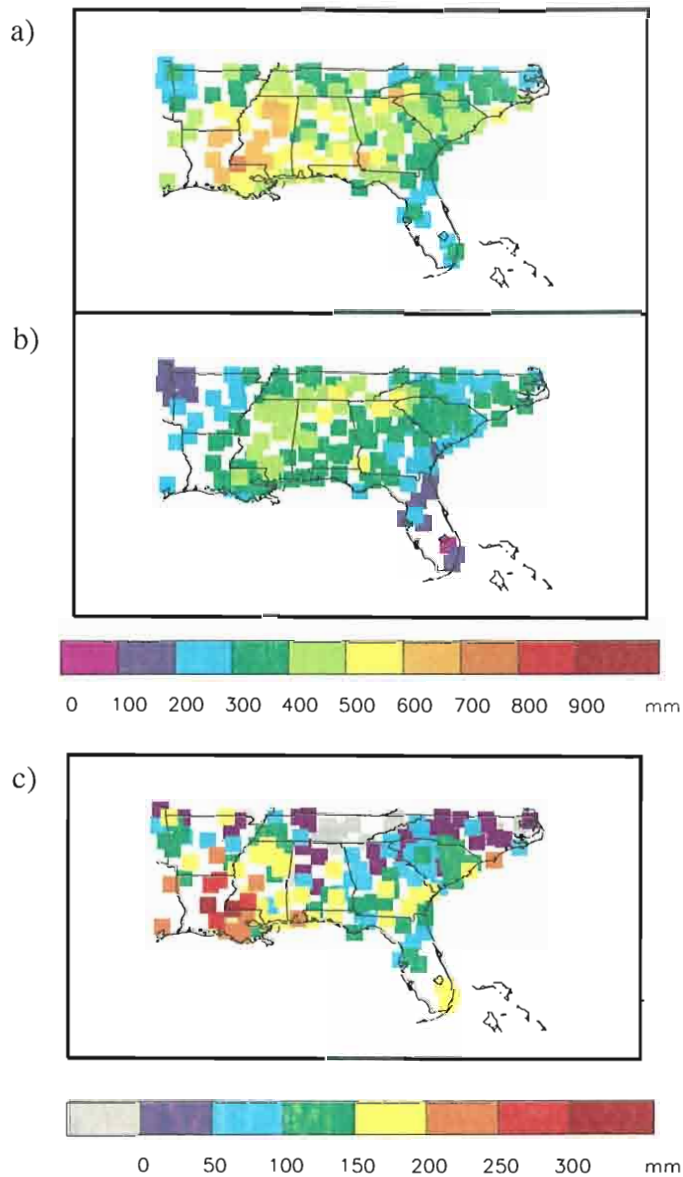


Fig. 8. USHCN total DJF precipitation (mm) for extreme warm (a) and cold (b) ENSO events and (c) extreme warm minus cold event precipitation totals. Figure (a) shows maximum in precipitation (> 600 mm) in Mississippi and Louisiana. In (a), a precipitation minimum (< 400 mm) occurs in the peninsula of Florida. In (b), a precipitation maximum (> 400 mm) occurs in Mississippi, Alabama, and Tennessee. Precipitation minima occur in the peninsula of Florida (< 300 mm) and in Arkansas (< 300 mm). Figure (c) shows a maximum (> 200 mm) in warm minus cold precipitation totals in Louisiana and Mississippi. Warm minus cold precipitation values < 0 are peninsula of Florida (< 300 mm) and in Arkansas (< 300 mm). Figure (c) shows a maximum (> 200 mm) in warm minus cold precipitation totals in Louisiana and Mississippi. Warm minus cold precipitation values < 0 are evident in most of Tennessee.

Further comparison of the model precipitation estimates to validate the rainfall over the ocean is necessary. The CPC Merged Analysis of Precipitation (CMAP; Xie and Arkin 1997) contains global monthly averaged precipitation totals on a 2.5°x 2.5° grid obtained by merging rain gauge and 5 satellite estimates (GPI, OPI, SSM/I scattering, SSM/I emission, and MSU). The data are available from 1979-1998. Since the data span only 19 years, any year in which a warm event occurred is selected for comparison. These years are 1982-83, 1986-87, 1987-88, 1991-92, and 1997-98. The winter season total precipitation values for the study region from CMAP also show two precipitation maxima (Fig. 9). The double-ensemble precipitation maxima are shifted eastward of the location of the CMAP precipitation maxima. These maxima have larger magnitudes than the observed maxima, likely due to the bias in the model to produce too much precipitation over ocean. However, the double-ensemble's overall pattern of larger precipitation amounts over the Gulf of Mexico and along the Gulf coast into Louisiana, Alabama, and Mississippi, as well as larger amounts of precipitation off the coast of the Carolinas is shown in the CMAP data.

4.2.2 Cold Event

Two maxima are evident (Fig. 10) in the double-ensemble cold event precipitation estimates. The most precipitation is located off the coast of North and South Carolina, and the western Gulf of Mexico stretching into Alabama and Mississippi. The winter season total precipitation estimates for a cold ENSO event show less precipitation in most locations within the southeastern United States than the precipitation estimates for a warm event precipitation in most locations within the southeastern United States than the precipitation estimates for a warm event.

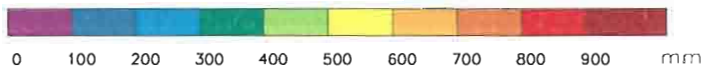
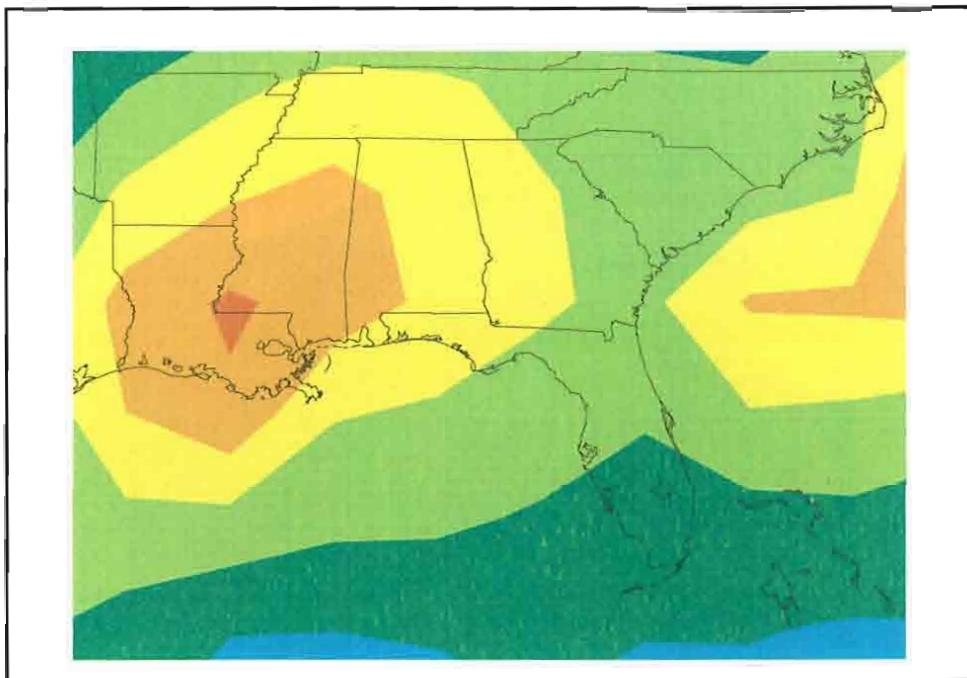


Fig. 9. CMAP total DJF precipitation (mm) for ENSO warm events (1982-83, 1986-87, 1987-88, 1991-92, 1997-98). A precipitation maximum (> 600 mm) is evident in Louisiana, Mississippi, and western Alabama. Another precipitation maximum (> 600 mm) occurs off the coast of the Carolinas. A relative minimum occurs in the peninsula of Florida (< 500 mm).

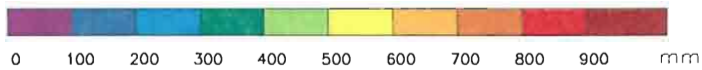
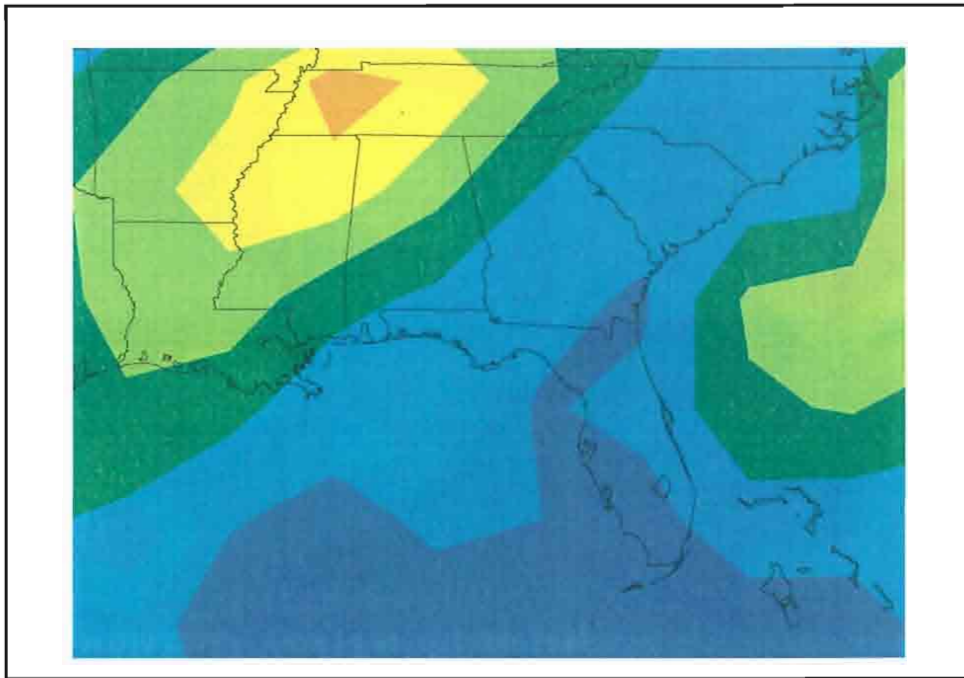


Fig. 11, Same as figure 9, but for ENSO cold event of 1988-89. A precipitation maximum (> 500 mm) is centered around western Tennessee. A band of < 200 mm of precipitation extends from the Gulf of Mexico across Florida, into Georgia, South Carolina, and North Carolina.

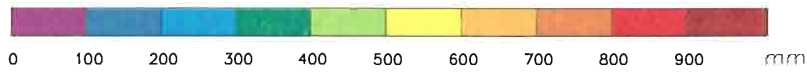
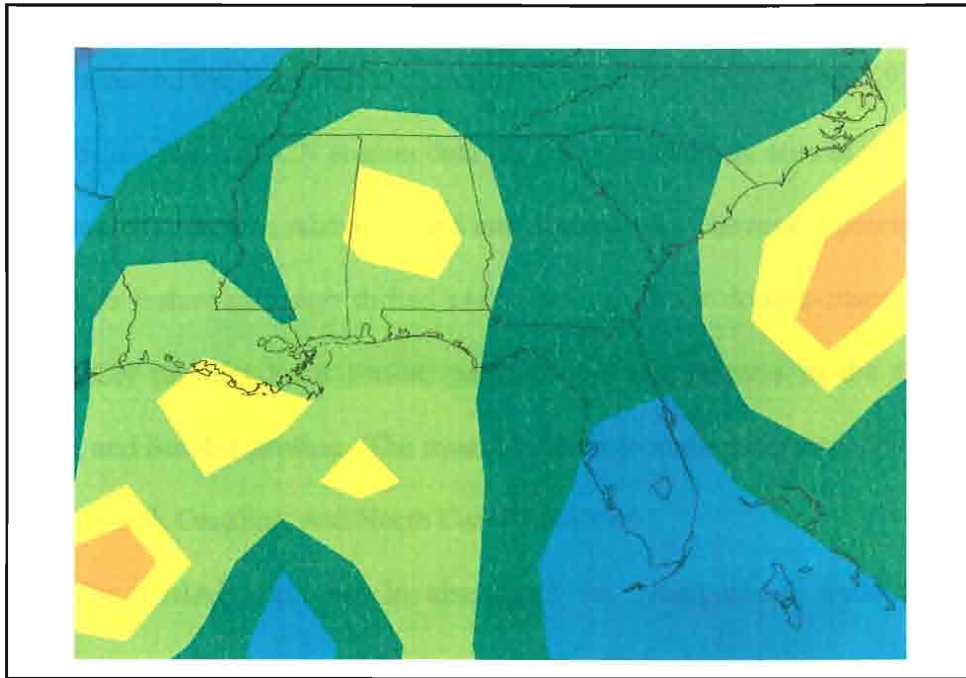


Fig. 10. Same as figure 7, but for an ENSO cold event. Precipitation maximums (> 500 mm) occur in the Gulf of Mexico, central Alabama, and off the coast of the Carolinas. A relative minimum (< 400 mm) occurs in Florida.

The double-ensemble cold event precipitation estimates (Fig. 10) are compared with USHCN station data (Fig. 8b) and CMAP data (Fig. 11). The three strongest cold events (based on the JMA index) are selected from the USHCN data: 1970-71, 1973-74, and 1975-76. The USHCN station data (Fig. 8b) indicate an area of greater precipitation in Mississippi, northern Alabama, and into Tennessee. The model precipitation estimates capture this feature although shifted southward. Both the double-ensemble estimates and the USHCN product have similar patterns and magnitudes in the states of Florida, Georgia, and South Carolina. The model appears to underestimate a drier patch along the Georgia, South Carolina, and North Carolina coasts.

The CMAP data set is also used for comparison with double-ensemble precipitation estimates for an ENSO cold event. Only the cold event of 1988-89 (Fig. 11) occurs within the CMAP period. It shows maximum values of precipitation over the Atlantic Ocean off the coast of the Carolinas similar to the model estimated precipitation. However, the magnitudes are again greater in the model precipitation estimates due to a bias in the model precipitation over the ocean. There are major differences between these cold event precipitation patterns, which is to be expected with only one observation based sample.

4.2.3 Relative Standard Deviations

Standard deviations of double-ensemble precipitation totals are calculated and divided by the double-ensemble averaged warm and cold event precipitation totals. This value indicates the relative standard deviation in the double-ensemble forecasts (Fig. 12). For an ENSO warm event, most of the southeastern United States has a spread of 10-15%. The primary exception is south Florida with a spread of 20-25%. For cold ENSO

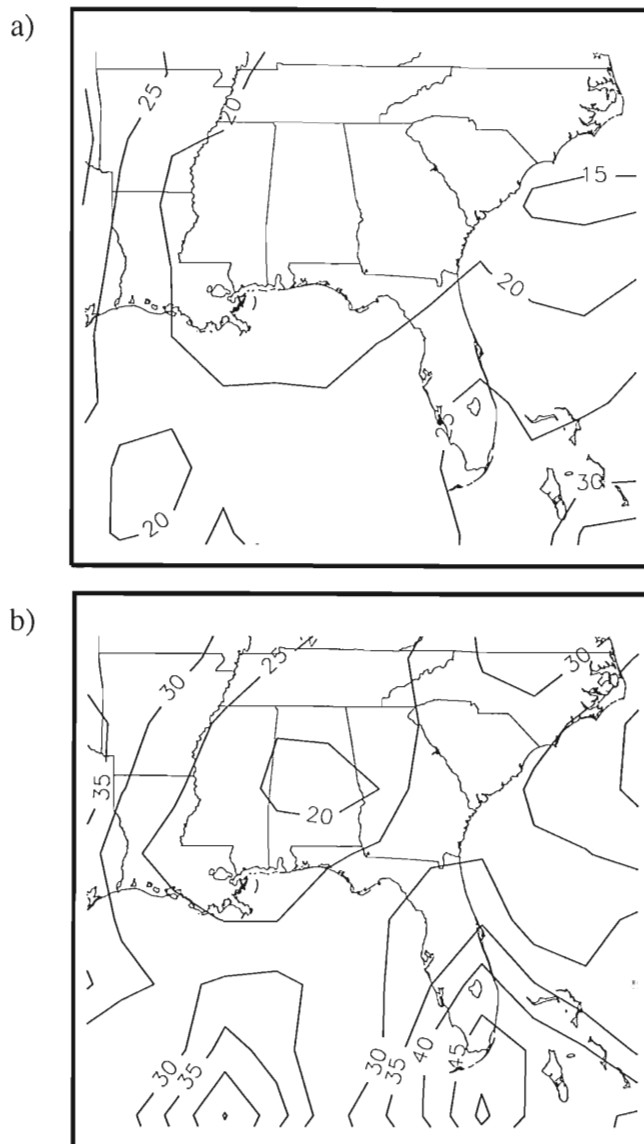


Fig. 12. Relative standard deviations (%) of ENSO (a) warm and (b) cold event double ensemble precipitation estimates. Relative standard deviations are calculated by determine the standard deviations of each extreme event and dividing by the mean for that event. Warm event relative standard deviations are $< 25\%$ for land areas, and cold event relative standard deviations are $< 30\%$ for most land areas except for the peninsula of Florida. The double ensemble precipitation estimates show larger relative standard deviations for areas, and cold event relative standard deviations are $< 30\%$ for most land areas except for the peninsula of Florida. The double ensemble precipitation estimates show larger relative standard deviations for extreme ENSO cold events than warm events, largely due to the smaller cold event means

events, the spread relative spread is larger in most areas due to the smaller cold event means. The smallest relative spread occurs in central Alabama (20%). South Florida has the largest relative spread of 30-50%. Based on this information it can be said that these double-ensemble precipitation estimates have a relatively low, but not negligible, spread over land, validating the concept of applying double-ensemble method to investigate the atmosphere's response to extreme ENSO events.

4.3 Warm Event minus Cold Event Differences

The double-ensemble precipitation estimates for extreme warm and cold events are differenced to determine the "envelope" of atmospheric response from warm to cold ENSO events. Clearly, this difference (Fig. 13) is largest in the Gulf of Mexico and near the coast of South Carolina, with over 200 mm more precipitation is estimated to occur during a warm event than during a cold event. Based upon the model estimated precipitation totals, the difference in precipitation from warm to cold ENSO events decreases to the northwest into Tennessee and Arkansas where the FSUGSM estimates less than 100 mm difference during opposite extreme events. Likewise, towards southern Florida and the Bahamas, precipitation differences decrease to less than 150 mm more during a warm event than during a cold event. Overall, the double-ensemble warm minus cold precipitation differences estimate at least 50 mm more precipitation during a warm event winter than during a cold event winter throughout the entire southeast region.

These estimated precipitation differences from warm to cold events are also compared to the USHCN station and CMAP data sets. The extreme warm events of 1972-73 and 1982-83 and extreme cold events of 1970-71, 1973-74, and 1975-76 are compared to the USHCN station and CMAP data sets. The extreme warm events of 1972-73 and 1982-83 and extreme cold events of 1970-71, 1973-74, and 1975-76 are selected from the 52 years of USHCN station data in a comparison with the model

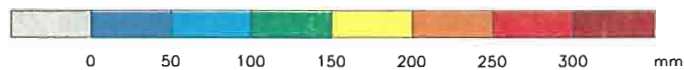
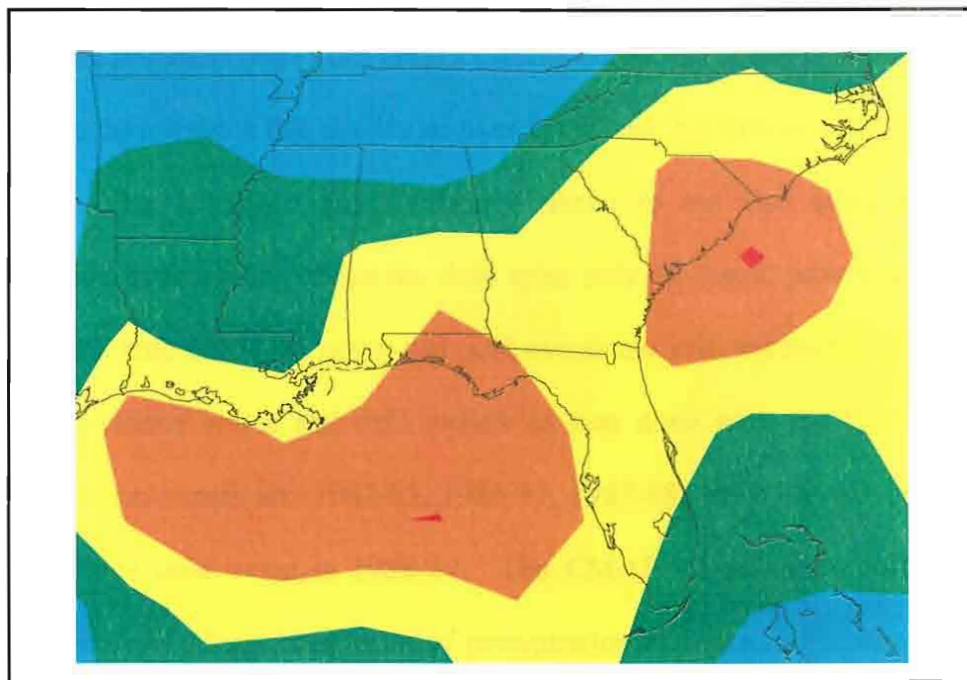


Fig. 13. Double ensemble warm minus cold event model precipitation (mm) differences for DJF. Maximums (> 200 mm) in precipitation differences occur in the Gulf of Mexico and the eastern portion of South Carolina into the Atlantic Ocean.

estimated precipitation differences. Most likely due to the small number of samples used, the USHCN station data shows (Fig. 8c) no distinct pattern other than a maximum in Louisiana primarily due to the 1982-83 warm event. The model estimated precipitation differences do not show this maximum over Louisiana, but instead show a maximum off the coast. The estimated precipitation differences are also compared to CMAP precipitation differences. Since the data span only 19 years, providing only 5 warm events and 1 cold event, all warm and cold events are selected from the data instead of choosing extreme warm and cold events as was done with the USHCN data. The available warm events are: 1982-83, 1986-87, 1987-88, 1991-92, and 1997-98 and the only available cold event is 1988-89. The CMAP warm minus cold precipitation differences show a large maximum of precipitation differences (greater than 250 mm) along the Gulf Coast (Fig. 14). A similar pattern is captured by the model precipitation estimates (Fig. 13), although it does not extend across southern Georgia and northern Florida as in the CMAP data. In both the CMAP differences (Fig. 14) and the USHCN differences (Fig. 8c), values less than zero are obtained in Tennessee indicating that this area does not receive more precipitation during warm event winters than cold event winters. The model estimated precipitation does not capture this feature but instead shows more precipitation throughout the entire southeast region during an average warm event winter than during an average cold event winter.

4.3.1 Relative Uncertainty in the Precipitation Mean Differences

The relative uncertainty in the mean difference from warm to cold events

--2

The relative uncertainty in the mean difference from warm to cold events

$\frac{\sigma^2}{\overline{P_w - P_c}}$ is determined by:

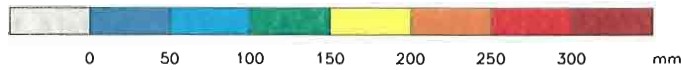
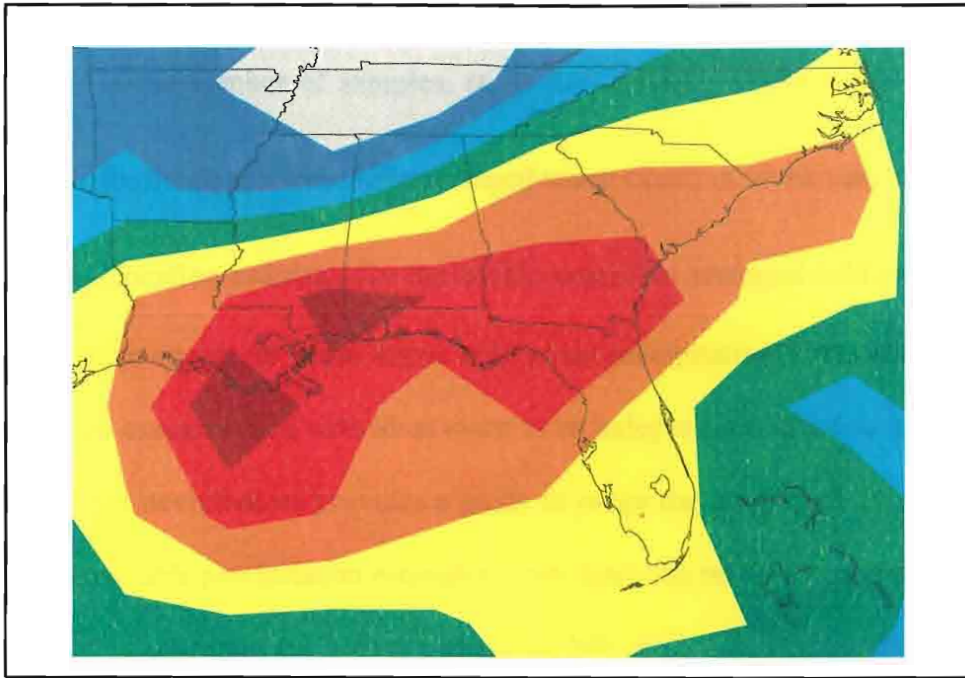


Fig. 14. CMAP warm minus cold DJF precipitation totals (mm). A large area of maximum (> 200 mm) warm minus cold precipitation differences extends across the Gulf coast, into northern and central Florida, and across much of Georgia and South Carolina.

$$\frac{\sigma_{\overline{P_w - P_c}}^2}{\overline{P_w} - \overline{P_c}} = \left(\frac{\sigma_w}{\sqrt{N}} \right)^2 + \left(\frac{\sigma_c}{\sqrt{N}} \right)^2, \quad (1)$$

where N is the number of samples, σ_w is the standard deviation of the precipitation estimates for the double-ensemble averaged warm event, σ_c is the standard deviation of the precipitation estimates for the double-ensemble averaged cold event, and $\overline{P_w} - \overline{P_c}$ is the double-ensemble warm minus cold event precipitation difference. Although this calculation assumes each individual event to be independent, which is not necessarily the case here, it nevertheless provides a guide to judge the magnitude of uncertainty in the double-ensemble precipitation estimates. Over land, the relative uncertainties in the mean precipitation estimates are between about 10-20% (Fig. 15). An uncertainty in the mean differences of approximately 20-25% occurs over Kentucky, Tennessee, and into Mississippi and Alabama. This area corresponds to the area which has negative warm minus cold event precipitation differences according to the CMAP (Fig. 14) and USHCN (Fig. 8c) data. This uncertainty in the mean differences of the double-ensemble precipitation estimates is too small to account for the fact that the model did not capture such negative differences shown by observations and satellite. However, the spread in the precipitation differences is within one standard deviation of the mean. This spread indicates that negative precipitation differences found in observations could be due to the small sample of observations available for comparison. The usefulness of the double-ensemble technique is clearly seen here by the lack of enough observation based samples. ensemble technique is clearly seen here by the lack of enough observation based samples.

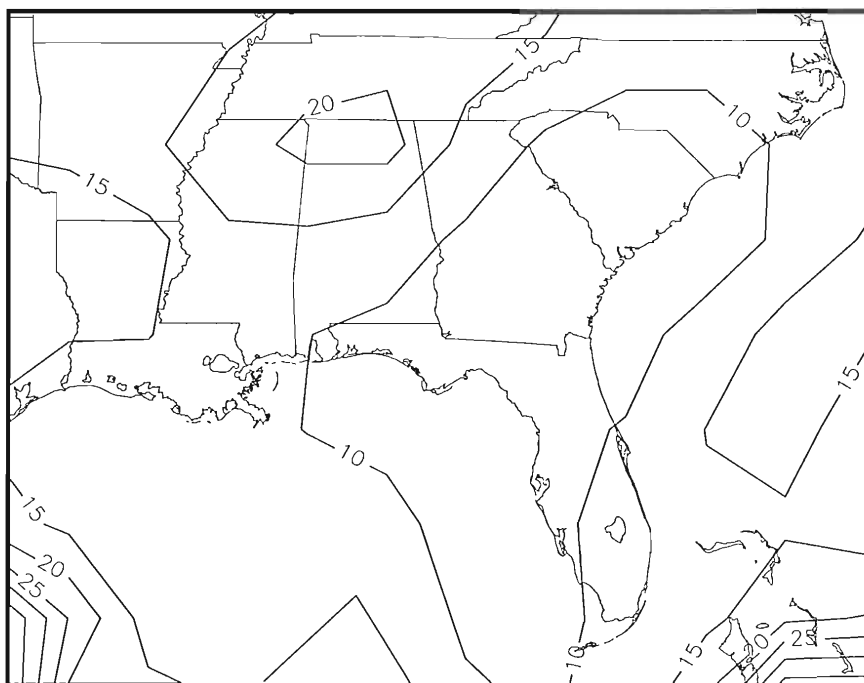


Fig. 15. Relative uncertainty (%) in the mean warm minus cold double ensemble precipitation differences. Maximum (> 40 %) uncertainty in the mean occurs at the southern corners of the region in the Gulf of Mexico and Atlantic Ocean. For land areas, maximum (> 15%) uncertainty in the mean occurs in Tennessee, stretching into northern Alabama and Mississippi.

5. CONCLUSIONS

Extreme warm and cold ENSO events are simulated from synthetic SSTs for the equatorial Pacific Ocean. Four warm and four cold events are used as boundary conditions for the FSUGSM with the purpose of investigating winter precipitation in the southeastern United States during extreme ENSO events. Teleconnections are known to exist between SSTs in the equatorial Pacific Ocean associated with ENSO and winter precipitation in the southeastern U.S. (Sittel 1994; Green 1996) due to altered 850 hPa and 300 hPa large-scale flow over the United States (Smith et al. 1998). This teleconnection is especially pronounced for extreme ENSO events. Therefore, extreme ENSO precipitation is investigated using a new double-ensemble technique. The double-ensembles are averages of model precipitation estimates for 10 different atmospheric initial conditions combined with synthetic SSTAs for the 4 warm and 4 cold events.

These double-ensemble precipitation estimates are obtained by changing only the initial conditions for the atmosphere and the SSTs in the equatorial Pacific Ocean. The precipitation estimates for the southeastern United States during extreme warm and cold events are in agreement with both station (USHCN) and satellite data (CMAP). The modeled precipitation is similar to CMAP and USHCN data in both spatial pattern and magnitude. The model estimated precipitation and observation show that on average the modeled precipitation is similar to CMAP and USHCN data in both spatial pattern and magnitude. The model estimated precipitation and observation show that on average the southeastern United States receives more precipitation during an ENSO warm event than

during an ENSO cold event. The uncertainty in the mean differences between warm and cold events is relatively low (10-20%) over land, reinforcing the applicability of this new double-ensemble technique.

Based upon the double-ensemble technique, an estimate of the envelope of atmosphere response in the southeastern United States for extreme ENSO events is determined. The maximum modeled precipitation in the southeastern United States during an extreme ENSO warm event winter did not exceed 475 mm. The minimum modeled precipitation in the southeastern United States during an extreme cold event winter is approximately 140 mm.

The double-ensemble technique is clearly useful in estimating the mean and the “envelope” of atmospheric responses from warm and cold ENSO events. Further studies, although requiring significantly more computer time, could be done using a higher resolution version of the FSUGSM, or even the regional version of this model, to more accurately resolve ocean vs. land problems, as well as areas where the Appalachian mountains play a large role in precipitation. Additionally, the double-ensemble technique could be applied to other atmospheric variables, as well as other regions of the globe to further study the global impacts of ENSO.

REFERENCES

- Arakawa, A., and W. H. Schubert, 1974: Interaction of a cumulus cloud ensemble with the large-scale environment. *J. Atmos. Sci.*, **31**, 674-701.
- Barnett, T. P., 1995: Monte Carlo climate forecasts. *J. Climate*, **8**, 1005-1022.
- Caron, J.M. and O'Brien, J.J., 1998: The Generation of Synthetic Sea Surface Temperature Data for the Equatorial Pacific Ocean. *Mon. Wea. Rev.*, **126**, 2809-2821.
- Chang, L. W. 1978: Determination of surface flux of sensible heat, latent heat, and momentum utilizing the bulk Richardson number. *Papers in Meteor. Res.*, **1**, 16-24.
- Cocke, S. and T. E. LaRow, 1999: Seasonal Prediction using a Nested Coupled Ocean-Atmospheric Regional Spectral Model (In press *Mon. Wea. Rev.*).
- Green, P. M., 1996: Regional Analysis of Canadian, Alaskan, and Mexican Precipitation and Temperature Anomalies for ENSO Impact. Tech. Rep. 96-7, Center for Ocean Atmospheric Prediction Studies, The Florida State University, 55 pp. [Available from COAPS, 2135 East Paul Dirac Drive, R. M. Johnson Bldg., Tallahassee, 32306]
- Hashvardan and T. G. Corsetti, 1984: Long-wave parameterization for the UCLA/GLAS GCM. NASA Tech. Memo 86072, Goddard Space Flight Center, Greenbelt, MD 20771, 52 pp.
- Japan Meteorological Agency, 1991: Climate charts of sea surface temperatures of the western north Pacific and the global ocean. Japan Meteorological Agency, Tokyo, Japan, 51 pp. [Available from Japan Meteorological Agency, 3-5 Otemachi-1, Chiyoda-Ku, Tokyo 100, Japan.]
- LaRow, T. E. and T. N. Krishnamurti, 1998: Initial conditions using a coupled ocean-atmosphere model. *Tellus*, **50A**, 76-94.
- Karl, T. R., C. N. Williams, Jr., F. T. Quinlan, and T. A. Boden., 1990: United States Historical Climatology Network (HCN) serial temperature and precipitation data. Environmental Science Division Publication No. 3404, 387 pp. [Available from Carbon Dioxide Information and Analysis Center, Oak Ridge National Laboratory, Oak Ridge, TN, USA.]
- Karl, T. R., C. N. Williams, Jr., F. T. Quinlan, and T. A. Boden., 1990: United States Historical Climatology Network (HCN) serial temperature and precipitation data. Environmental Science Division Publication No. 3404, 387 pp. [Available from Carbon Dioxide Information and Analysis Center, Oak Ridge National Laboratory, Oak Ridge, TN, USA.]

- Kanamitsu, M., K. Tada, K. Kudo, N. Sato and S. Isa, 1983: Description of the JMA operational spectral model. *J. Met. Soc. Japan*, **61**, 812-828.
- Kanamitsu, M., 1975: On numerical prediction over a global tropical belt. Report No. 75-1, Dept. of Meteorology, Florida State University, Tallahassee, Florida 32306, pp 1-282.
- Krishnamurti, T.N., 1995: Numerical Weather Prediction. *Annu. Rev. Fluid Mech.*, **27**, 195-224.
- Krishnamurti, T. N., J. Xue, H. S. Bedi, K. Ingles and D. Oosterhof, 1991: Physical Initialization for numerical weather prediction over the tropics. *Tellus*, **42AB**, 53-81.
- Lacis, A. A., and J.E. Hansen, 1974: A parameterization of the absorption of solar radiation in the earth's atmosphere. *J. Atmos. Sci.*, **31**, 118-133.
- Manobianco, J., 1988: On the observational and numerical aspects of explosive east coast cyclogenesis. Ph. D. Dissertation, The Florida State University, 361pp. [Available from the Dept. of Meteorology, The Florida State University, Tallahassee, FL., 32306].
- Pan, H. -L., and W. S. Wu 1994: Implementing a mass flux convection parameterization package for the MNC MRF model. *Preprints Tenth Conference on Numerical Weather Prediction*, Portland, Or, Amer. Meteor. Soc. 96-98.
- Rasmusson, E.M. and Carpenter, T.H., 1982: Variations in Tropical Sea Surface Temperature and Surface Wind Fields Associated with the Southern Oscillation/El Nino. *Mon. Wea. Rev.*, **110**, 354-384.
- Sittel, M. C., 1994: Marginal probabilities of the extremes of ENSO events for temperature and precipitation in the southeastern United States. Tech. Rep. 94-1, Center for Ocean Atmospheric Prediction Studies, The Florida State University, 55 pp. [Available from COAPS, 2135 East Paul Dirac Drive, R. M. Johnson Bldg., Tallahassee, 32306]
- Smith, S. R., P.M. Green, A. P. Leonardi, and J.J. O'Brien, 1998: Role of Multiple-Level Tropospheric Circulations in Forcing ENSO Winter Precipitation Anomalies. *Mon. Wea. Rev.*, **126**, 3102-3116.
- Smith, T. M., R. W. Reynolds, R. E. Livezey, and D. C. Stokes, 1996: Reconstruction of historical sea surface temperatures using empirical orthogonal functions. *J. Climate*, **9**, 1403-1420.
- SMITH, T. M., R. W. REYNOLDS, R. E. LIVEZEY, and D. C. STOKES, 1996: RECONSTRUCTION OF historical sea surface temperatures using empirical orthogonal functions. *J. Climate*, **9**, 1403-1420.
- Stenstrud, D. J., and E. Rogers, 1999: Using Ensembles for Short-Range Forecasting. *Mon. Wea. Rev.*, **127**, 433-446.

- Tiedke, M. 1984: The sensitivity of the time-mean large-scale flow to cumulus convection in the ECMWF model. *Workshop on Convection in large-scale numerical models* ECMWF, 28 Nov. – 1 Dec. 1983, 297-316. ECMWF, Shinfield Park, Reading RG2 9AX, UK.
- Whitaker, J. S. and Lough, A. F., 1998: The Relationship between Ensemble Spread and Ensemble Mean Skill. *Mon. Wea. Rev.*, **126**, 3292-3302.
- Xie, P. and Arkin, P.A., 1997: Global Precipitation: A 17-year Monthly Analysis Based on Gauge Observations, Satellite Estimates, and Numerical Model Outputs. *Bull. Amer. Met. Soc.*, **78**, 2539-2558.
- Zhang, Z. and T. N. Krishnamurti, 1999: A perturbation method for hurricane ensemble predictions. *Mon. Wea. Rev.*, **127**, 447-469.

BIOGRAPHICAL SKETCH

Degrees

M.S. Meteorology , anticipated December, 1999, The Florida State University, Tallahassee, FL.

B.S. Meteorology, 1998, The Florida State University, Tallahassee, FL.

B.S. Computer and Information Sciences, 1998, The Florida State University, Tallahassee, FL.

Experience

1996-present: Center for Ocean-Atmospheric Prediction Studies (COAPS)/ Florida State University, Graduate/Undergraduate Research Assistant.

1995-96: Florida State University Meteorology Department Weather Station, Student Assistant.

Summer 1996: Florida State University Meteorology Department, Dr. Sharon Nicholson, Undergraduate Research Assistant.

Summer 1995: NASA Summer Institute on Atmospheric and Hydrospheric Sciences, Student Intern.

Honors

Honors

Chi Epsilon Pi, National Meteorology Honor Society.

Upsilon Pi Epsilon, National Computer Science Honor Society.

Personal Information

Born 10 April 1975, Jackson, Mississippi.